JOURNAL OF GEOPHYSICAL RESEARCH, VOL. 100, NO. B11, PAGES 22,533–22,542, NOVEMBER 10, 1995

Toward a better understanding of the Lowrie-Fuller test

Song Xu and David J. Dunlop

Department of Physics, Erindale College, University of Toronto, Mississauga, Ontario, Canada

Abstract. We develop a theory of acquisition and alternating field (AF) demagnetization of anhysteretic remanence (ARM) and saturation isothermal remanence (SIRM) in multidomain (MD) grains in order to better understand the Lowrie-Fuller test. Our theory shows that the relative stabilities of low-field ARM and high-field SIRM against AF demagnetization are determined by the distribution $f(h_c)$ of microcoercivity h_c in a sample, as found earlier by Bailey and Dunlop. When $f(h_c)$ is nearly constant, weak-field ARM is more resistant to AF demagnetization than SIRM. In contrast, when $f(h_c)$ varies exponentially or is a Gaussian distribution, SIRM is more AF resistant than ARM. These contrasting stability trends are conventionally called single-domain (SD)-type and MD-type Lowrie-Fuller results, respectively, but in reality, both types occur in the MD size range. We propose instead the descriptive terms L-type result (low-field remanence, i.e., ARM, more stable) and H-type result (high-field remanence, i.e., SIRM, more stable). The Lowrie-Fuller test does not distinguish one type of domain structure from another, but it does depend indirectly on grain size. We show that the distribution $f(h_c)$ in a given sample is determined primarily by the grain size d and the dislocation density ρ. A nearly constant $f(h_c)$ occurs in grains with small d and/or ρ, but a Gaussian $f(h_c)$ is approached with increasing d and/or ρ. The transition from L-type to H-type behavior in the Lowrie-Fuller test occurs at a critical grain size $d_t \approx 2/(\rho w)$, where w is the domain-wall width. The lower the dislocation density, the larger the transition size in the Lowrie-Fuller test. This simple relationship explains the increase in the transition size from about 5-10 μm observed for crushed magnetite grains to ≈ 100 μm for hydrothermally grown magnetites, which have lower dislocation densities than crushed grains.

Introduction

The Lowrie-Fuller test [*Lowrie and Fuller*, 1971] has been widely used in paleomagnetism to distinguish whether the carriers of remanence in a rock sample are mainly single-domain (SD) or multidomain (MD) grains. As proposed by *Lowrie and Fuller* [1971], the relative stability against alternating field (AF) demagnetization of thermal remanence (TRM) carried by SD grains should decrease with an increasing inducing field, H_o, but the AF stability should increase for MD grains. Since TRM approaches saturation isothermal remanence (SIRM) when H_o is sufficiently large, a simple form of the test is to compare the relative AF stabilities of TRM and SIRM: For SD grains, TRM is more resistant to AF than SIRM, and for MD grains the opposite occurs. In practice, one may replace TRM by anhysteretic remanence (ARM) and observe a similar trend [*Dunlop et al.*, 1973; *Johnson et al.*, 1975].

Grains larger than the critical SD size also exhibit SD-type behavior in the Lowrie-Fuller test. For example, *Hartstra* [1982] and *Bailey and Dunlop* [1983] observed SD-type behavior for crushed magnetite grains ≲ 10 μm (Figure 1) (the critical SD size of magnetite is ~ 0.1 μm). This result is usually attributed to so-called pseudo-single-domain (PSD) behavior of small MD grains. Recently, a surprising result was reported by *Heider et al.* [1992], who observed SD-type behavior up to 100 μm for their hydrothermally grown magnetites (Figure 1). The result is surprising not only because 100 μm is far beyond the reasonable PSD size range for magnetite but also because the grown magnetites used by Heider et al. are magnetically softer than crushed magnetites, according to hysteresis measurements [*Heider et al.*, 1987]. Therefore one would expect the PSD to MD transition size for the hydrothermal magnetites to be smaller than for the crushed magnetites, rather than larger.

The underlying mechanism of the Lowrie-Fuller test is still not clear, in part because of our poor understanding of the origin of magnetic stability in PSD grains. *Bailey and Dunlop* [1983] suggested that the result of the Lowrie-Fuller test is controlled mainly by the shape of the AF demagnetization curve, which is determined by both the internal demagnetizing field and the distribution of intrinsic microcoercivities in a sample. They found that an AF demagnetization curve that decays superexponentially usually gives the SD-type result, and in contrast, one that decays subexponentially usually gives the MD-type. However, it is not clear how this changeover relates to such intrinsic factors as grain size and defect state.

Failure of domain-wall nucleation, leaving a grain in a metastable SD-like state, might also be responsible for the SD-type behavior of PSD grains. Following *Fuller* [1984], TRM in PSD grains may be controlled largely by a few grains in SD-like states that have difficulty nucleating walls. In contrast, when SIRM is produced after applying a saturating field, a relatively large population of grains remain in SD-like states, but wall nucleation can occur in a relatively small AF. Consequently, SIRM may be less stable to AF demagnetization than TRM, leading to the SD-type Lowrie-Fuller result. It is hard to imagine, however, that hydrothermal magnetites ≈ 100 μm in size can remain in metastable SD-like states of remanence. Furthermore, it is not at all clear why the hydrothermal magnetites of *Heider et al.* [1992], with a low dislocation density, should have a larger transition size from SD-type to MD-type Lowrie-Fuller results than crushed magnetites, as shown in Figure 1.

Paper number 95JB02154.
0148-0227/95/95JB-02154$05.00

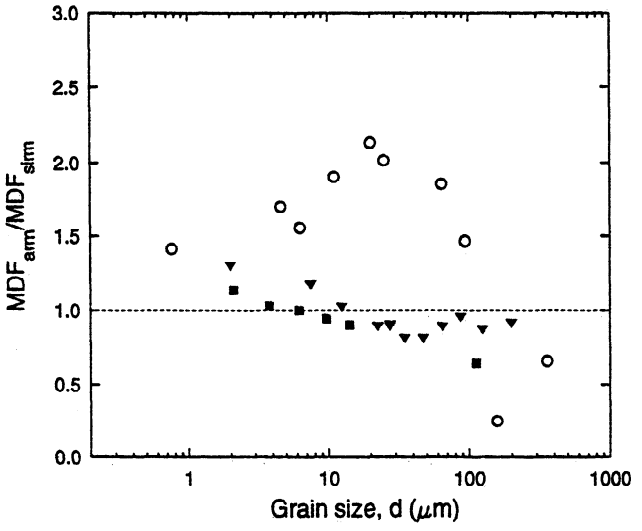

Figure 1. The variation of the ratio of the median destructive field (MDF) of ARM (MDF_{arm}) to MDF_{sirm} with grain size d for crushed magnetite grains from *Hartstra* [1982] (triangles) and *Bailey and Dunlop* [1983] (squares) and for hydrothermally grown magnetite grains from *Heider et al.* [1992] (circles). The transition size d_t defined by $MDF_{arm}/MDF_{sirm} = 1$ is ≈ 10 μm for Hartstra's samples, ≈ 5 μm for Bailey and Dunlop's samples, and ≈ 100 μm for Heider et al.'s samples.

In this paper, we model theoretically the behavior of PSD and MD grains in the Lowrie-Fuller test. In particular, we relate the result of the Lowrie-Fuller test to grain size and dislocation density of a sample. This is done by first considering the effect of grain size and dislocation density on the distribution of microcoercivities that pin walls and then calculating the relative stabilities of ARM and SIRM against AF demagnetization. In a later section, we discuss the effect of wall nucleation on the Lowrie-Fuller result.

Microcoercivity Distributions in MD Grains

The microcoercivity distribution plays an important role in determining the relative stability of remanence against AF demagnetization in the Lowrie-Fuller test. Early MD TRM theory [*Néel*, 1955; *Stacey*, 1962; *Schmidt*, 1973, 1976] was developed using a series of identical, closely spaced energy barriers that impede the motion of walls. The resulting microcoercivity h_c, which is a measure of the maximum slope of a given energy barrier, has a single value, independent of TRM intensity. Consequently, when TRM is induced in a large H_o, we have a large demagnetizing field (∝ TRM intensity) but the same h_c. This results in a TRM whose AF stability decreases as H_o increases. The Lowrie-Fuller test for MD grains should therefore be of SD-type, a paradoxial conclusion at odds with the intent of the Lowrie-Fuller test. More realistic microcoercivity distributions were considered by *Bailey and Dunlop* [1983]. By combining theory and experiment, they concluded that the Lowrie-Fuller test is of SD-type or MD-type depending on whether the microcoercivity distribution $f(h_c)$ varies slower or faster than an exponential decay function.

The distribution of h_c in real grains depends on both grain size and defect density. For example, consider dislocations, which are the most likely source of wall pinning in magnetite [*Xu and Merrill*, 1992; *Moskowitz*, 1993]. In a cubic grain of size d, the total number n_t of dislocation lines is ρd^2, ρ being the dislocation density (number per unit area). When n_t is small, the pinning of individual walls is likely by individual dislocations. Then the resulting $f(h_c)$ represents the distribution of h_c associated with individual dislocations, which is expected to be relatively constant over a range of h_c from zero to a maximum value $2H_c$ (H_c is the mean of this random distribution). The variation of h_c can be caused by such factors as the length of a dislocation and the angle between a dislocation line and the wall plane [e.g., *Xu and Merrill*, 1989]. In contrast, when n_t is large, individual walls are likely to be pinned by many dislocations simultaneously. In this case, the pinning of individual walls is determined by the fluctuation in the number of dislocations from place to place within a grain. Then $f(h_c)$ approaches a Gaussian distribution.

As an illustration of the transition of $f(h_c)$ from a random (i.e., a flat) distribution to a Gaussian distribution with increasing n_t, we calculated $f(h_c)$ for an ensemble of cubic grains with given d and ρ. In the calculation, each grain in the ensemble contains $n_t = \rho d^2$ dislocations whose strengths in pinning a wall and locations within the grain are randomly distributed. The resulting $f(h_c)$ should be close to random for the grains with small d and/or ρ in which each wall interacts only with individual dislocations. However, with increasing d and/or ρ, we should see $f(h_c)$ approaching a Gaussian distribution. The detailed calculation is given in the appendix.

Calculated $f(h_c)$ distributions are plotted versus h_c/H_c in Figure 2. H_c is the mean microcoercivity defined as

$$H_c = \int_0^\infty h_c f(h_c)\, dh_c. \tag{1}$$

In all cases shown in Figure 2, the shape of $f(h_c)$ is well characterized by a single parameter n, given by ρwd, which represents the average number of dislocations in a wall. For n = 0.05 « 1 (Figure 2b), the distribution is essentially level with $f(h_c) \approx 1/(2H_c)$ ($0 \le h_c < 2H_c$). With increasing n, $f(h_c)$ changes gradually from random to Gaussian; $f(h_c)$ is already Gaussian by $n = 5$. The dislocation densities used in the calculation were $\rho = 10^{11}$, 10^{12}, and $10^{13}m^{-2}$ for n = 0.1, 1, and 10 in the 10-μm grains and for n = 0.5, 5, and 50 in the 50-μm grains, respectively, and $\rho = 10^{10}m^{-2}$ for n = 0.05 in the 50-μm grains. For crushed magnetites, ρ typically ranges from 10^{12} to $10^{14}m^{-2}$, and for the hydrothermally grown magnetites, ρ was reported to be $3 \times 10^{10}m^{-2}$ [*Heider et al.*, 1987].

The transition of $f(h_c)$ from a random to Gaussian distribution is illustrated further in Figure 3. In Figure 3, the reduced mean microcoercivity is normalized to the value of H_c for a random distribution. For $n < 2$, the reduced H_c is close to 1 and $f(h_c)$ is close to random. When $n > 2$, H_c is $\propto \sqrt{n}$ and $f(h_c)$ is Gaussian. For a given ρ, the transition size d_t from random to Gaussian is therefore given by

$$d_t \approx \frac{2}{\rho w}. \tag{2}$$

As will be shown later, d_t plays an important role in determining the SD-type to MD-type transition in the Lowrie-Fuller test.

In subsequent sections, we examine the effect of $f(h_c)$ on AF stability of ARM and SIRM. We use three types of $f(h_c)$, given as follows:

Random
$$f(h_c) = \frac{1}{2H_c} \qquad h_c \le 2H_c, \tag{3a}$$

Gaussian
$$f(h_c) = \frac{2}{\pi H_c} \exp\left[-\frac{1}{\pi}\left(\frac{h_c}{H_c}\right)^2\right], \tag{3b}$$

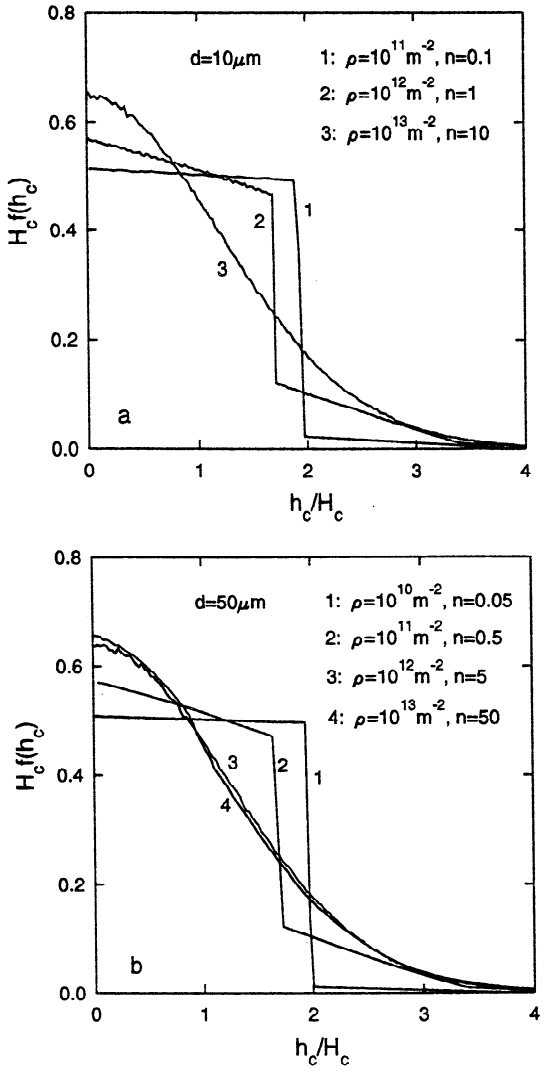

Figure 2. The distributions of microcoercivities calculated for (a) 10-μm and (b) 50-μm grains with different dislocation densities, where n is the average number of dislocations in a wall and ρ is the dislocation density. When n is small, the microcoercivity distribution $f(h_c)$ varies relatively slowly with microcoercivity h_c. When n is large, $f(h_c)$ approaches a Gaussian distribution.

Exponential
$$f(h_c) = \frac{1}{H_c} \exp\left(-\frac{h_c}{H_c}\right). \tag{3c}$$

The exponential distribution is included because of its importance in the study by *Bailey and Dunlop* [1983].

It is actually more convenient in the calculation to use the cumulative distribution $F(h_c)$, defined as

$$F(H_c) = \int_{h_c}^{\infty} f(h_c)dh_c, \tag{4}$$

which is directly related to the AF demagnetization curve by replacing the argument h_c of F by $\tilde{H}$ ($\tilde{H}$ is peak AF). Specifically,

$$F(h_c) = \left(1 - \frac{h_c}{2H_c}\right), \; 1 - \mathrm{erf}\left(\frac{h_c}{\sqrt{\pi}H_c}\right), \; \exp\left(-\frac{h_c}{H_c}\right) \tag{5}$$

for random, Gaussian, and exponential distributions of h_c given in (3), respectively. In (5), erf is the error function. The three types of $F(h_c)$ given in (5) are plotted in Figure 4 and resemble AF demagnetization curves. In both (3) and (5), the mean microcoercivity H_c may be taken as the bulk coercivity of a sample [*Xu and Merrill*, 1990].

Weak-Field ARM

We will first consider weak-field ARM, in which the wall makes only a single jump away from or toward the demagnetized state. In weak-field ARM, we assume that the wall is displaced a distance x from its demagnetized ($M = 0$) position over a single energy barrier into the neighbouring potential well. However, the internal demagnetizing field will drive the wall some distance up the side of this well toward the $M = 0$ well, with the result that its maximum displacement x_{max} is always is less than λ, the wavelength of energy barriers or the spacing between the bottoms of adjacent wells. The ARM will be AF demagnetized when the wall makes a single Barkhausen jump toward the demagnetized state. The same approach was used by *Bailey and Dunlop* [1983].

The requirement for using this approach is that the maximum wall displacement x_{max} in the ARM state is smaller than the average wavelength λ of the energy barriers in the given grain. We can relate x_{max} to the ARM biasing field H_o as follows. During ARM acquisition, the equilibrium wall position x_{eq} is determined by the balance between H_o and the demagnetizing field $NM_{eq} = 2x_{eq}NM_s/d$, where M_s is the saturation magnetization and N is the demagnetizing factor, hereafter taken to be constant for any given grain. The actual x in the ARM state will be $\leq x_{eq}$ as a wall tends to fall back toward its demagnetized position upon the removal of H_o. Thus, taking $x_{max} = x_{eq}$, we have

$$\frac{x_{max}}{d} = \frac{H_o}{2NM_s} \tag{6}$$

Stacey [1963] gave a statistical estimate of $\lambda = \sqrt{3}w$, and *Xu and Merrill* [1989] found $\lambda = 5w$ for the most effective pinning of a wall

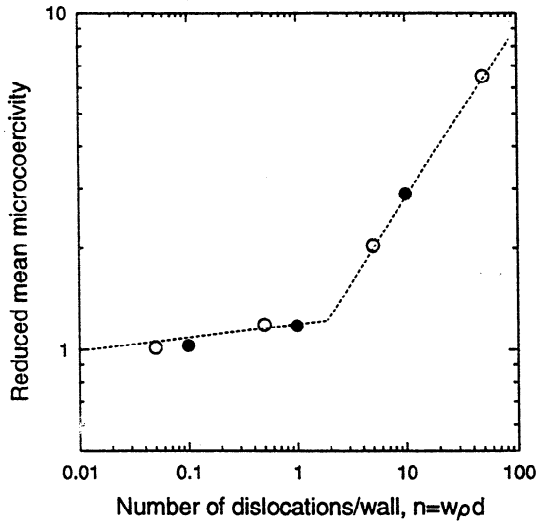

Figure 3. Mean microcoercivity H_c as a function of n. The reduced values of H_c plotted are normalized to the H_c value for a random distribution of h_c. When $n > 2$, $H_c \propto \sqrt{n}$ (i.e., slope 1/2), as expected for a Gaussian distribution. When $n < 2$, the reduced H_c is close to 1 and the corresponding $f(h_c)$ is close to a random distribution.

by an energy barrier. As an estimate, we take $\lambda \approx w$, and since $x_{max} < \lambda$, we have from (6)

$$H_o d < 2wNM_s . \quad (7)$$

Inequality (7) indicates the ranges of H_o and d in which the single energy barrier approach is reasonable. For magnetite (M_s = 480 kA/m, N = 1/3 for equidimensional grains and w = 0.1 μm), we require $H_o \leq$ 4mT, when d = 10 μm or $H_o \leq$ 0.4 mT, when d = 100 μm.

The ARM intensity M_{arm} of an individual grain is always equal to or less than the induced magnetization $M_{eq} = H_o/N$. When H_o is turned off, the wall will jump back to its demagnetized position in the $M = 0$ well if h_c is less than the demagnetizing field $NM_{eq} = H_o$; that is, when $h_c < H_o$. If $h_c > H_o$, the wall will remain pinned in the neighboring well, giving an ARM intensity of H_o/N. Here the movement of a wall around the bottom of a local energy well is assumed to be small and is therefore ignored. For an ensemble of grains with a distribution of h_c, the total intensity of ARM is obtained by integrating over $f(h_c)$:

$$M_{arm} = \frac{H_o}{N} \int_{H_o}^{\infty} f(h_c)dh_c = \frac{H_o}{N} F(H_o). \quad (8)$$

In reality, it is not just H_o but the sum of H_o and the AF, $\tilde{H}$, that drives the walls. $\tilde{H}$ can have a magnitude >> H_o, but positive and negative values are equally probable. Thus only the net field H_o is effective, and (8) gives the statistical average value of ARM.

Consider now the AF demagnetization of the ARM given in (8). During AF demagnetization, h_c works against both the demagnetizing field $NM_{eq} = H_o$ and the peak AF $\tilde{H}$. If $h_c < \tilde{H} + H_o$, the wall is unpinned and the corresponding ARM is AF demagnetized (with the single energy barrier approach). Otherwise, the wall remains pinned and the ARM intensity is unchanged. Thus, by replacing H_o by $\tilde{H} + H_o$ in the lower integral limit in (8), we obtain the total ARM intensity as a function of $\tilde{H}$ for an ensemble of grains. A normalized AF demagnetization curve of ARM is therefore given by

$$\frac{M_{arm}(\tilde{H})}{M_{arm}(0)} = \frac{F(H_o + \tilde{H})}{F(H_o)} \quad (9)$$

where $M_{arm}(0)$ is the ARM before AF demagnetization as given by (8).

Therefore, within the weak field range, an exponential distribution of h_c given by (3c) results in $M_{arm}(\tilde{H})/M_{arm}(0) = \exp(-\tilde{H}/H_c)$ for any H_o, which is a null Lowrie-Fuller test. Any superexponential distribution of h_c, such as random and Gaussian distributions given by (3a) and (3b), respectively, gives a SD-type Lowrie-Fuller result, and in contrast, any subexponential distribution gives a MD-type result. The same conclusion was reached by *Bailey and Dunlop* [1983].

Within the weak-field range, the difference in AF stabilities of two ARMs induced in H_{01} and H_{02}, respectively, is actually very small; it is of the order of $(H_{02} - H_{01})/H_c$, as can be seen by expanding (9) in a Taylor series in terms of H_o/H_c. If we neglect all higher-order terms of H_o/H_c in the expansion, we have from (9)

$$\frac{M_{arm}(\tilde{H})}{M_{arm}(0)} \approx F(\tilde{H}). \quad (10)$$

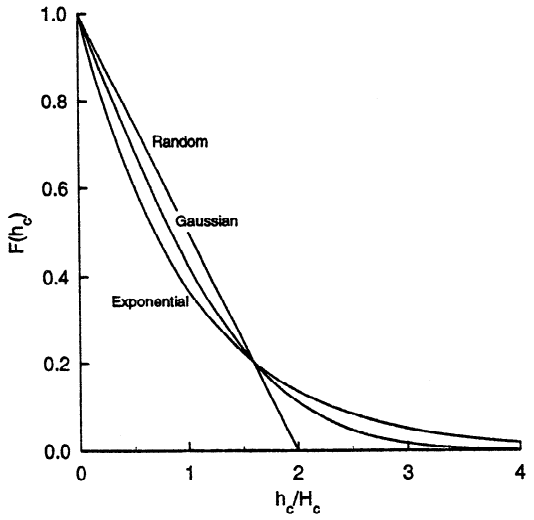

Figure 4. The cumulative distributions of microcoercivities given in equation (5). $F(h_c)$ resembles an AF demagnetization curve.

Thus the normalized AF demagnetization curve coincides with the cumulative distribution of h_c, as given by (5) and plotted in Figure 4.

We can determine the median destructive fields MDF_{arm} from (5) and (10). They are H_c, $0.845H_c$, and $0.693H_c$ for random, Gaussian, and exponential distributions, respectively. These values of MDF_{arm} will be compared in the following section to the corresponding MDF_{sirm}. In the above, we did not consider the magnetic screening effect of soft walls. The screening will reduce the intensity of a remanence by a screening factor α ($\leq$ 1) but will increase the MDF by the same factor [*Moon and Merrill*, 1986; *Xu and Dunlop*, 1993]. Because of the screening, the values of MDF/H_c we obtain will be smaller than actual experimental values for magnetite samples, particularly for samples that contain large grains and/or have a small dislocation density [*Xu and Dunlop*, 1993]. However, we will be mainly concerned with MDF_{arm}/MDF_{sirm}, which is a measure of the Lowrie-Fuller result and should not be significantly affected by the screening.

Strong-Field ARM and SIRM

SIRM can be considered as a saturated ARM induced in a sufficiently large H_o. When H_o is large, individual walls will encounter multiple energy barriers during AF demagnetization. For any given H_o the maximum number of energy barriers that a wall may encounter is

$$m = \frac{M_{eq}}{\Delta M} = \frac{H_o}{N\Delta M}, \quad (11)$$

where M_{eq} is the equilibrium magnetization with H_o turned on and ΔM is the change in magnetization when a wall undergoes a Barkhausen jump across an energy barrier. We take ΔM to be constant for a grain of given size. The acquisition of ARM is modeled by assuming that after the AF is reduced to zero but before H_o is turned off, the magnetization of a grain is equal to M_{eq} and the wall is at the m th barrier. When H_o is turned off, the wall may be driven back by the demagnetizing field to the i th barrier, where $i \leq$

m, and $M_{arm} \leq M_{eq}$. During AF demagnetization, the wall is driven back further and a complete demagnetization occurs when the wall reaches $i = 0$.

In our model, the difference between the acquisition of ARM and that of isothermal remanence (IRM) induced in the same H_o is in the wall position before H_o is turned off: During the acquisition of IRM, the wall usually cannot reach the m th barrier but is blocked at an intermediate barrier that has $h_c > H_o$ (unless H_o is a saturating field). In contrast, during the acquisition of ARM, the wall is able to cross all intermediate barriers with the aid of the AF and always reaches the m th barrier.

Because of the distribution of H_c, the position of a particular wall or the value of i in the ARM state has to be determined statistically. For a wall to be pinned at the i th barrier, a necessary condition is that all the barriers from $i + 1$ to m are unable to pin the wall. The sufficient condition is that h_c associated with the i th barrier is larger than the demagnetizing field $iN\Delta M$. Statistically, we can write the probability p_i that a wall is pinned by the i th barrier as

$$p_i = \prod_{j=i+1}^{m} (1-p_j) \int_{iN\Delta M}^{\infty} f(h_c)dh_c = \prod_{j=i+1}^{m} (1-p_j)F(iN\Delta M), \quad (12)$$

where p_j is the probability that the wall is pinned by the j th barrier and therefore $(1 - p_j)$ is the probability that the wall is not pinned. The product in (12) represents the probability that the wall is not pinned by any of the barriers between $i + 1$ and m. The function F in (12) represents the requirement that h_c must be larger than the demagnetizing field $iN\Delta M$ at the i th barrier, so that the wall will not be driven back to the barrier $i - 1$. Equation (12) is a recurrence formula and is started with p_m given by

$$p_m = F(H_o), \quad (13)$$

which is the probability that the wall is pinned at the m th barrier (i.e., for $h_c \geq NM_{eq} = H_o$). Consequently, the total ARM intensity for an ensemble of grains is

$$M_{arm} = \Delta M \sum_{i=1}^{m} i p_i, \quad (14)$$

where $i\Delta M$ is the magnetization when a wall is pinned at the i th barrier. In (14), M_{arm} is dependent implicitly on H_o through p_i. When H_o is sufficiently large, M_{arm} approaches M_{sirm}, as will be seen below.

For a given $f(h_c)$, an ARM acquisition curve can be calculated using (12) to (14). An example is shown in Figure 5. One adjustable parameter in the calculation is $H_c/(N\Delta M)$, taken to be 10 in the example shown in Figure 5. This parameter may be taken as a grain size indicator. Now $\Delta M \propto 1/d$, but H_c decreases slower than $1/d$ as seen from bulk coercivity data as a function of grain size [e.g., *Dunlop*, 1986]. Therefore the value of $H_c/(N\Delta M)$ increases with increasing grain size.

For a given $H_c/(N\Delta M)$, both the saturation field of ARM and the SIRM intensity are largest for an exponential $f(h_c)$ and the smallest for a random $f(h_c)$, as seen in Figure 5. This trend results from the fact that with multiple energy barriers, both the saturation field and the SIRM intensity are determined mainly by the largest h_c among the m barriers that individual walls encounter. That is, they are determined mainly by the microcoercivities in the tail region of a given $f(h_c)$ or equivalently $F(h_c)$. The tail is largest for an exponential $f(h_c)$ and smallest for a random $f(h_c)$ among the three types of $f(h_c)$ considered (see Figure 4).

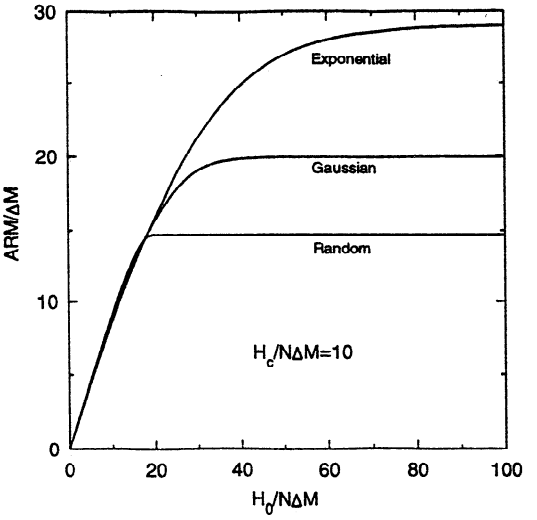

Figure 5. ARM acquisition curves calculated using equation (14) for the three types of $f(h_c)$. ARM is normalized to the change in magnetization, ΔM, when a wall undergoes a Barkhausen jump, and the DC biasing field, H_o, is normalized to the change in internal demagnetizing field, $N\Delta M$, resulting from ΔM.

It is interesting to note that the MDF_{arm} values obtained in the previous section vary in the opposite way: MDF_{arm} is smallest for an exponential $f(h_c)$ and largest for a random $f(h_c)$. At the first glance, this is inconsistent with what one might expect: a sample with a small MDF_{arm} should be more easily saturated, or vice versa. This apparent inconsistency can be understood by noting that MDF_{arm} determined from (10) is a measure of the median value of $f(h_c)$, while the saturation field is a measure of the maximum h_c in the distribution. For a given type of $f(h_c)$, the two parameters do vary coherently with H_c, or with grain size as in most real samples. However, this is not necessarily the case when $f(h_c)$ changes from one type to the other, as we see in Figure 4.

Consider now the AF demagnetization of the ARM given by (14). After AF demagnetization at a peak field $\tilde{H}$, the probability that a wall is pinned at any given energy barrier decreases, because h_c now has to work against not only the demagnetizing field but also $\tilde{H}$. At the i th barrier in particular, the probability q_i that a wall is pinned can be written, following (12), as

$$q_i = \prod_{j=i+1}^{m} (1-q_j)F(iN\Delta M + \tilde{H}). \quad (15)$$

In (15), the product represents the fractional number of walls that have jumped to the i th barrier from barriers with $j > i$ after AF demagnetization, and the function F represents the condition that h_c must be sufficiently large to pin a wall at the i th barrier. The main difference between (12) and (15) is in the argument of F. The recurrence of (15) is started with

$$q_m = F(H_o + \tilde{H}) \quad (16)$$

which is similar to (13). Consequently, the normalized AF demagnetization of ARM is given by

$$\frac{M_{arm}(\tilde{H})}{M_{arm}(0)} = \frac{\sum_{i=1}^{m} i q_i}{\sum_{i=1}^{m} i p_i} \quad (17)$$

where $M_{arm}(0)$ is the ARM before AF demagnetization. For a given $f(h_c)$, $M_{arm}(\tilde{H})/M_{arm}(0)$ in (17) can be determined numerically as a function of H_o/H_c and $\tilde{H}/H_c$, with one adjustable parameter $H_c/(N\Delta M)$ which serves as a grain size indicator, as discussed above.

The AF demagnetization curve of SIRM can be calculated by setting H_o to a sufficiently large value that $M_{arm}(0)$ is saturated. In the cases shown in Figure 5, $M_{arm}(0)$ is well saturated at $H_o/H_c = 10$.

The multiple energy barrier model developed above is different from the model used by *Bailey and Dunlop* [1983] in examining the Lowrie-Fuller test in MD grains. The model we have developed is a statistical model, in which the pinning of a wall at a particular energy barrier requires $h_c > NM$ (+ $\tilde{H}$ after AF demagnetization) with h_c obeying a given distribution function. In contrast, the model developed by *Bailey and Dunlop* [1983] is an equilibrium model, in which the wall position and thus M are determined by an equilibrium condition $h_c = NM$ (+ $\tilde{H}$). In an equilibrium model, applying $\tilde{H} > h_c - NM$ implies a complete demagnetization for a given wall. However, in our statistical model, the application of the same $\tilde{H}$ simply pushes a wall to the next energy barrier and does not necessarily mean a complete demagnetization. Thus a wall in our model is given choices for a range of h_c values as the wall moves back to its demagnetized position and therefore is more likely to exhibit a MD-type Lowrie-Fuller result as we will see in the next section. Once the problem is reduced to a single energy barrier, the two models are almost identical, and they give the same result, as in the case of weak-field ARM discussed in the previous section.

Finally, it should be pointed out that in our model, an implicit assumption is that the h_c values associated with individual energy barriers are independent of each other; therefore the probability of having a microcoercivity h_c at any location in a grain is the same as at any other location, all being represented by $f(h_c)$. The same assumption was used in calculating the distribution of h_c earlier in the paper.

Comparison Between Weak-Field ARM and SIRM

In this section, we compare the AF demagnetization curves of weak-field ARM and SIRM. Figure 6 shows the normalized AF demagnetization curves of ARM and SIRM determined respectively from (10) and (17) for $H_c/(N\Delta M) = 10$. The Lowrie-Fuller test is of SD type for the random distribution but MD-type for the exponential and Gaussian distributions.

This changeover from SD-type to MD-type can be understood as resulting from the competition between the demagnetizing field and microcoercivity. Following the argument by *Lowrie and Fuller* [1971], the demagnetizing field H_d is larger for SIRM than for weak-field ARM. On the other hand, a wall in the SIRM state is more likely to encounter a large h_c when the wall moves toward a demagnetized state during AF demagnetization. The largest h_c that a given wall can possibly encounter is determined largely by microcoercivities in the tail region of a given $f(h_c)$; the tail is largest for an exponential $f(h_c)$ and smallest for a random $f(h_c)$, as we discussed in the previous section. For a random distribution, therefore, the demagnetizing field effect is dominant and SIRM demagnetizes more readily than weak-field ARM (SD-type result). For Gaussian and exponential distributions, the maximum microcoercivity encountered by a wall is more important, and SIRM is accordingly harder to erase than weak-field ARM (MD-type result).

The relative AF stabilities of ARM and SIRM also vary with the parameter $H_c/(N\Delta M)$ and thus with grain size (Figure 7). For a given $f(h_c)$, MDF_{arm}/MDF_{sirm} decreases with increasing $H_c/(N\Delta M)$.

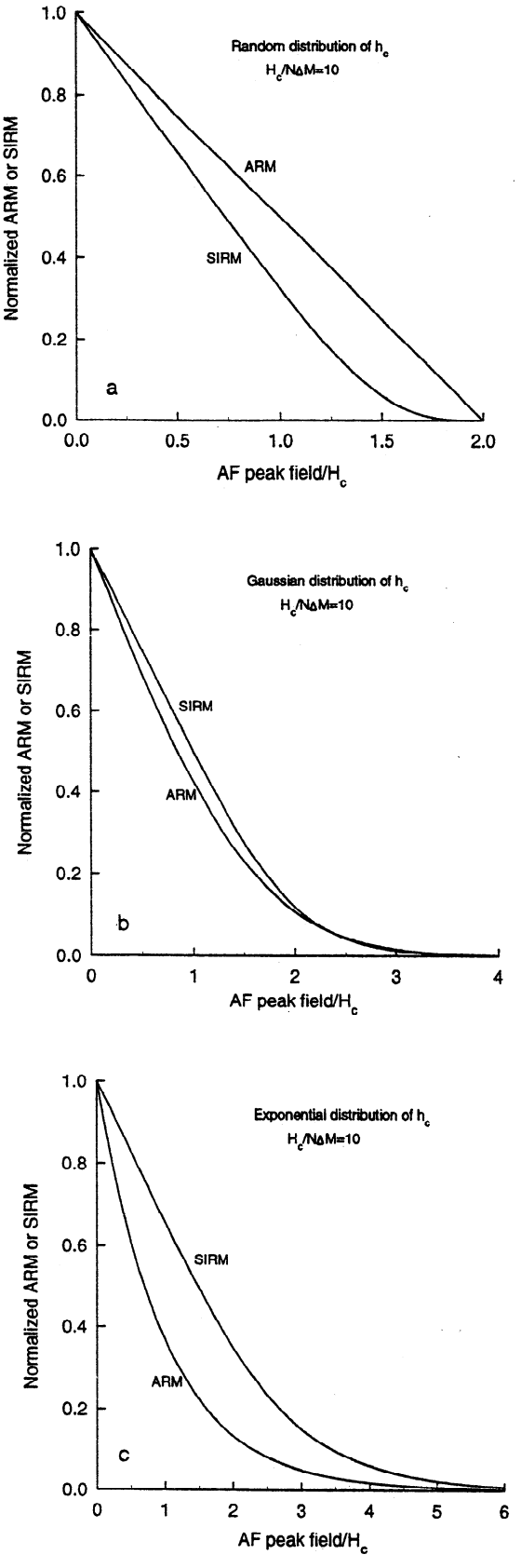

Figure 6. Normalized AF demagnetization curves of weak-field ARM and SIRM calculated from equations (10) and (17), respectively, for the three types of $f(h_c)$. The Lowrie-Fuller test is of SD-type for a random distribution, while it is of MD-type for Gaussian and exponential distributions.

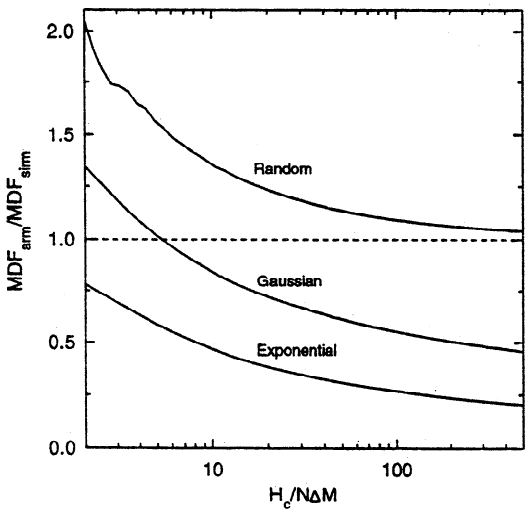

Figure 7. The ratio of MDF_{arm}/MDF_{sirm} as a function of $H_c/(N\Delta M)$, and thus grain size, for the three types of $f(h_c)$. $H_c/(N\Delta M)$ is mean microcoercivity H_c normalized to the change in internal demagnetizing field $N\Delta M$, resulting from a Barkhausen jump. The relationship of this parameter to grain size is explained in the text. The Lowrie-Fuller test is of SD-type for a random distribution and of MD-type for an exponential distribution. For a Gaussian distribution, it is of MD-type for magnetite grains $\geq$ 1 μm (see discussion in text).

i.e. with increasing grain size. Note that MDF_{arm}/H_c is actually a constant for a given $f(h_c)$ (see calculations following (10)). Thus the patterns seen in Figure 7 reflect an increase in MDF_{sirm}/H_c with increasing $H_c/(N\Delta M)$. This increase occurs because a large $H_c/(N\Delta M)$ (H_c being constant) implies that a wall at SIRM has to cross a large number of energy barriers and thus is more likely to encounter a large h_c before reaching its demagnetized position.

For a random distribution, the Lowrie-Fuller test is always of SD-type with MDF_{arm}/MDF_{sirm} decreasing to the asymptotic value 1 as $H_c/(N\Delta M)$ increases. In contrast, it is always of MD-type for an exponential distribution, contrary to the previous result by *Bailey and Dunlop* [1983]. For a Gaussian distribution, the Lowrie-Fuller test changes from SD-type to MD-type at $H_c/(N\Delta M) \approx 5$. Here, the value $H_c/(N\Delta M)$ can be seen as representing an average number of energy barriers encountered or Barkhausen jumps made by a wall from its SIRM to demagnetized position. If we take $2w$ as the average wavelength of the energy barriers, we have the MD-type for magnetite grains with grain size $d > 5x2w = 10w \approx 1$ μm, provided that $f(h_c)$ in the grains is Gaussian.

Understanding the Lowrie-Fuller Test in Real Samples

The result of the Lowrie-Fuller test depends strongly on the distribution of microcoercivities in grains in a given sample, as illustrated in Figures 6 and 7. Two important parameters that determine the h_c distribution are grain size d and dislocation density ρ. In small grains with a low dislocation density, individual walls interact with individual dislocations, and thus we expect $f(h_c)$ to vary slowly with h_c. With increasing d and/or ρ, the number of dislocations that a wall encounters increases. In the limit, $f(h_c)$ approaches a Gaussian distribution. The changeover in $f(h_c)$ is actually quite sharp as shown in Figure 3, and it occurs at $d_t\rho w \approx 2$ (equation (2)). Thus, as a first-order approximation, the result of the Lowrie-Fuller test is determined by

$$\text{SD-type} \qquad d\rho w < 2$$

$$\text{MD-type} \qquad d\rho w > 2 \qquad (18)$$

The lower the dislocation density, the larger the transition size in the Lowrie-Fuller test.

The simple relationship given in (18) provides an explanation for the experimental data shown in Figure 1. For hydrothermally grown magnetite grains, the dislocation density is low, and therefore the transition size is large, compared to the crushed magnetite grains. A quantitative estimate using (18) gives a transition size $d_t < 20$ μm for crushed magnetite grains with $\rho > 10^{12}$ m^{-2} ($w = 0.1$ μm), which is comparable to the observed values in Figure 1. For the hydrothermally grown magnetites, $\rho = 3x10^{10}$ m^{-2} [*Heider et al.*, 1987] corresponds to $d_t \approx 700$ μm, which is larger than ~100 μm observed (Figure 1). The overestimate may be attributed to the assumption of the wall area $\approx d^2$ used in deriving (18), which is a reasonable approximation only for small grains.

Effect of Domain Nucleation

In the theory developed above, the number of domains in a given grain is assumed to be constant. It is possible, however, that the number of domains in a grain changes during AF demagnetization or between ARM and SIRM states. It has been found experimentally [*Halgedahl and Fuller*, 1983; *Halgedahl*, 1991] that the number of domains in some titanomagnetite grains is different in different remanence states. In particular, the number of domains is usually smallest when in an SIRM state and increases after AF demagnetization, indicating that domain nucleation takes place during AF demagnetization of SIRM.

Suppose that the AF stability of ARM (or SIRM which is an ARM induced in a saturating H_o) is determined predominantly by the critical AF, $\tilde{H}_n$, that triggers domain nucleation. At a given nucleation site in a grain, we can write

$$\tilde{H}_n = h_a - H_d, \qquad (19)$$

where h_a is the anisotropy field and H_d is the demagnetizing field. The value of h_a is dependent on the anisotropy imposed by crystal defects as well as the magnetocrystalline anisotropy and exchange energies at the nucleation site. At a given nucleation site, h_a can reasonably be assumed to be constant, independent of the number of domains or domain wall displacement. The role of h_d in (19) is the same in domain nucleation as in wall pinning; it works against h_a (in domain nucleation) or h_c (in wall pinning) and tends to bring a grain closer to a demagnetized state. Following (19), when an ARM is induced in a large H_o, H_d is large and therefore $\tilde{H}_n$ is small. Thus, if domain nucleation is a predominant factor in determining the AF stability of ARM, we expect a SD-type Lowrie-Fuller result. The same conclusion was reached by *Fuller* [1984], based on consideration of domain nucleation in grains in SD-like metastable states.

Therefore domain nucleation may provide an alternative explanation of the SD-type Lowrie-Fuller result observed in MD grains of magnetite in the PSD size range (1-10 μm). If so, the transition observed in Figure 1 for crushed magnetites around 10 μm would mark the changeover in the dominant coercivity mechanism from nucleation in the smaller grains to wall pinning in larger grains. Particles that contain walls but which have difficulty in forming additional walls, as well as metastable SD particles, could be nucleation controlled. Nucleation would also account for the initial

plateau in some PSD AF demagnetization curves. The threshold for AF demagnetization would be set by nucleation.

The very large transition size (≈ 100 μm) observed in hydrothermally grown magnetites is probably not due to nucleation, however. The 100-μm hydrothermal magnetites have extremely low M_{sirm}/M_s values, which are unlikely to be associated with nucleation. Also because of the relatively low dislocation density, we expect that the average anisotropy field h_a will be larger but H_c will be smaller for the grown magnetites than for crushed grains of similar size. Thus we expect the coercivity to be governed by wall pinning.

How Useful Is the Lowrie-Fuller Test?

The Lowrie-Fuller test was intended as a quick method of distinguishing between SD and MD carriers of natural thermal remanence. The test was based on measurements made at opposite extremes of the magnetite size spectrum. *Lowrie and Fuller* [1971] observed that in millimeter-sized single crystals, course polycrystalline aggregates and ≈250-μm sieved crystal fragments, strong-field TRM was more stable to AF demagnetization than weak-field TRM. Previously published data [*Rimbert*, 1959; *Dunlop and West*, 1969] showed that the opposite was true for single-domain magnetite (≤ 0.1 μm). It was therefore natural to associate these AF characteristics with MD and SD grains respectively, although just why MD and SD grains should behave in these ways remained contentious [*Dunlop and West*, 1969; *Schmidt*, 1976].

To be useful in paleomagnetism, the test must have discriminating power in the intermediate-size magnetites commonly found in rocks. Lowrie and Fuller had pointed out a possible gray area: grains larger than critical SD size but too small to contain well-formed domain walls. *Dunlop et al.* [1973] and *Johnson et al.* [1975] demonstrated that in fact the test (now modified to use ARM instead of TRM) gave a SD-type result for magnetites and maghemites well above critical SD size. Later, *Hartstra* [1982] and *Bailey and Dunlop* [1983] showed that magnetite grains as large as 10 μm still gave SD-type tests, in spite of having MD structure [e.g., *Heider et al.*, 1988].

It would have been logical at this point to abandon SD-like and MD-like as descriptions of observed AF trends. This did not happen, for several reasons.

1. Hysteresis properties and TRM intensities of magnetite showed gradual decreases over a broad size range extending up to about 10 μm [*Parry*, 1965], above which they were more or less constant. This was taken to be a confirmation of *Stacey*'s [1962, 1963] ideas about pseudo-single-domain (PSD) behavior in MD grains, with the PSD-MD threshold being ≈10 μm.

2. Magnetite grains around 10 μm in size were sometimes observed to remain in metastable SD states, especially in SIRM, but to nucleate walls in small fields during demagnetization [*Boyd et al.*, 1984]. These could be mechanisms for SD-like AF responses.

3. Magnetite grains of 10 μm size are still small enough to plausibly carry paleomagnetically stable and reliable remanence. Thus, even though the reason for a changeover in Lowrie-Fuller characteristics around this size was unclear, the test was still of practical utility.

This picture of the Lowrie-Fuller test as a discriminator between PSD magnetites, with stable SD-like remanence, and MD magnetites, with highly mobile walls and unstable remanence, became untenable when it was discovered that magnetites with low internal stress have size-dependent hysteresis properties [*Heider et al.*, 1987] and yield SD-type Lowrie-Fuller tests [*Heider et al.*, 1992] in grains as large as 100 μm (see Figure 1). These grains are only slightly smaller than the 250-μm magnetites whose AF response defines the MD end-member in the Lowrie-Fuller test. Equilibrium domain widths of ≈30 μm are observed in magnetites of this size [*Özdemir and Dunlop*, 1993]. Accordingly one would expect metastable SD states to be rare, and none have been reported. The 100 μm magnetites are very soft to AF demagnetization, and it is doubtful that they carry any trustworthy paleomagnetic remanence. The Lowrie-Fuller test, in low-stress magnetites, discriminates between two classes of large, soft grains; it works at the wrong end of the grain size scale, paleomagnetically speaking.

The Lowrie-Fuller test does not reflect domain structure per se. Grains in metastable SD states could account for a SD-like AF response in ≈10-μm magnetites, but they are unlikely to do so in ≈100-μm magnetites. Domain nucleation during AF demagnetization would tend to produce a SD-type test, but wall motion, not wall nucleation, should govern AF response in low-stress magnetites. We propose replacing the terms "SD-type" and "MD-type", which imply a well-understood connection between AF response and domain state, by "L-type" (low-field remanence more stable) and "H-type" (high-field remanence more stable), which describe what is actually observed in the test.

What then causes L-type and H-type responses in conventional MD grains, i.e., those in which walls move but are not created or annihilated? There are three factors: (1) the microcoercivity spectrum, which changes from a random to a Gaussian distribution as increasing grain size d and/or dislocation density ρ cause wall pins to change from a single defect to multiple defects; (2) the internal demagnetizing field; and (3) the wall displacement (high-field remanences push walls past many pinning sites, with a higher probability of encountering strong pinning). None of these factors is closely correlated with the number of domains. Even the role of grain size is indirect, because it is the product ρd, not d alone, that governs the microcoercivity distribution.

The single most important factor is the change of $f(h_c)$ from random to Gaussian as ρd increases. A random distribution always yields an L-type test (Figures 6a and 7), whereas a Gaussian distribution produces an H-type test (Figures 6b and 7). (In principle, a Gaussian distribution can produce an L-type test if d is below ≈1 μm (Figure 7) but provided $\rho \le 2\times10^{13}\mathrm{m}^{-2}$, $n=\rho wd \le 2$ and a random distribution prevails (Figure 3).) For reasonable dislocation densities, grain size has to be quite large to produce wall pinning by several dislocations simultaneously, to form a Gaussian microcoercivity distribution $f(h_c)$ and result in an H-type test. This explains the rarity of H-type tests in real rocks [*Lowrie and Fuller*, 1972; *Dunlop*, 1983].

Does the Lowrie-Fuller test have any practical utility? The answer is yes, with two provisos.

1. It must be clearly understood that the test results do not directly indicate domain structure. Many different structures, including "true" MD grains, can give a so-called SD-type (or L) test.

2. Comparisons must be made within a suite of rocks with similar states of internal stress. In general, an H-type test is grounds for rejecting a sample, but an L-type test is not necessarily proof of paleomagnetic stability. More information is required about the stress state of the magnetite grains and their size distribution. Unfortunately, this information is difficult to obtain.

Finally, we note that little is understood, experimentally or theoretically, about the AF responses of minerals other than magnetite and maghemite or their correlation with hysteresis and domain structure. High-titanium titanomagnetite (TM60), hematite, and pyrrhotite are prime candidates for investigation, particularly TM60 because of the rich variety of studies of domain nucleation and metastable states in this mineral [*Halgedahl and Fuller*, 1983; *Halgedahl*, 1991].

Conclusions

1. MD grains may exhibit either an L (or SD-type) or an H (or MD-type) result in the Lowrie-Fuller test, depending on the type of microcoercivity distribution $f(h_c)$ in the grains, as suggested earlier by *Bailey and Dunlop* [1983]. If $f(h_c)$ is approximately a random distribution, an L-type test results. In contrast, if $f(h_c)$ is Gaussian, an H-type test results.

2. The transition size d_t from the L-type to the H-type test result varies with the defect density. For dislocations, $d_t \approx 2/(\rho w)$, where ρ is the dislocation density and w is the wall width. Thus d_t increases with decreasing ρ, as observed (Figure 1). A quantitative estimate gives $d_t \leq 20$ μm for crushed magnetites with $\rho \geq 10^{12}\text{m}^{-2}$, comparable to the values observed. The value calculated for hydrothermally grown magnetites is $d_t \approx 700$ μm, which is larger than the ~100 μm observed, probably because of an overestimate of the wall area used in our calculation.

3. SD-type behavior is expected for grains in which AF stability is controlled by domain nucleation. Although this mechanism provides an alternative explanation for the SD-type behavior observed for <10 μm crushed magnetites, domain nucleation fails to explain the experimentally observed increase in the transition size d_t with decreasing dislocation density.

4. The Lowrie-Fuller test does not diagnose domain structure, but in a suite of rocks of similar stress state, it is a useful indicator of relative grain size and likely paleomagnetic stability.

Appendix: Calculation of the Microcoercivity Distribution

The following steps were taken in the calculation of the microcoercivity distribution $f(h_c)$ for an ensemble of cubic grains with a grain size d and a dislocation density ρ:

1. The number of dislocations n_t in each grain was taken to be ρd^2. The pinning strength of each dislocation was chosen randomly between -1 and +1, where the ± sign represents the sign of the Burgers vector of a dislocation. Here, the unit and maximum magnitude of the pinning strength are unimportant, because the resulting h_c is always plotted by normalizing to the mean microcoercivity H_c.

2. The location of each dislocation in a given size grain was also chosen randomly between 0 to d.

3. Given a distribution of n_t dislocations following steps 1 and 2, the magnitude of h_c at any given location in a grain was taken to be equal to the sum of the pinning strengths of any dislocations in the vicinity $\pm w$ of that location, where w is the wall width and $2w$ is the approximate interaction range between a 180° wall and a single dislocation [*Xu*, 1989]. We took $w = 0.1$ μm as in magnetite. The magnitude of h_c was calculated at intervals of $2w$ from 0 to d.

4. A statistical distribution $f(h_c)$ was obtained by repeating steps 1 to 3 for a large number of grains, all having the same grain size and dislocation density but different distributions of dislocation locations and strengths. The actual number of grains used for obtaining $f(h_c)$ was $2.5\text{x}10^{18}/(\rho d)$, where ρ and d are in units of m^{-2} and μm, respectively. It ranges from 5000 for 50-μm grains with $\rho = 10^{13}\text{m}^{-2}$ ($n = 50$ in Figure 2b) to $2.5\text{x}10^6$ for 10-μm grains with $\rho = 10^{11}\text{m}^{-2}$ ($n = 0.1$ in Figure 2a).

Finally, it should be pointed out that the distribution of the pinning strengths of dislocations in real grains can be more complex than the random distribution we used in step 1; it will depend on the distributions of the orientations of dislocation lines and Burgers vectors with respect to the wall plane. However, a random distribution is a good first order approximation for grains in which the dislocation lines and Burgers vectors have no particular favored direction.

Acknowledgments. We have benefitted greatly from discussions with Ronald Merrill. Helpful reviews by Susan Halgedahl, an anonymous referee, and the associate editor were much appreciated. This research was supported by the Natural Sciences and Engineering Research Council of Canada through grant A7709 to D.J.D.

References

Bailey, M. E., and D. J. Dunlop, Alternating field characteristics of pseudo-single-domain (2-14 μm) and multidomain magnetite, *Earth Planet. Sci. Lett., 63,* 335-352, 1983.

Boyd, J. R., M. Fuller, and S. Halgedahl, Domain wall nucleation as a controlling factor in the behavior of fine magnetic particles in rocks, *Geophys. Res. Lett., 11,* 193-196, 1984.

Dunlop, D. J., Determination of domain structure in igneous rocks by alternating field and other methods, *Earth Planet. Sci. Lett., 63,* 353-367, 1983.

Dunlop, D. J., Hysteresis properties of magnetite and their dependence on particle size: A test of pseudo-single-domain remanence models, *J. Geophys. Res., 91,* 9569-9584, 1986..

Dunlop, D. J., and G. F. West, An experimental evaluation of single domain theories, *Rev. Geophys., 7,* 709-757, 1969.

Dunlop, D. J., J. A. Hanes, and K. L. Buchan, Indices of multidomain magnetic behavior in basic igneous rocks: Alternating field demagnetization, hysteresis, and oxide petrology, *J. Geophys. Res., 78,* 1387-1393, 1973.

Fuller, M., On the grain size dependence of the behaviour of fine magnetic particles in rocks, *Geophys. Surv., 7,* 75-87, 1984.

Halgedahl, S. L., Magnetic domain patterns observed on synthetic Ti-rich titanomagnetite as a function of temperature and in states of thermoremanent magnetization, *J. Geophys. Res., 96,* 3943-3972, 1991.

Halgedahl, S. L., and M. Fuller, The dependence of magnetic domain structure upon magnetization state with emphasis upon nucleation as a mechanism for pseudo-single-domain behavior, *J. Geophys. Res., 88,* 6505-6522, 1983.

Hartstra, R. L., A comparative study of the ARM and I_{sr} of some natural magnetites of MD and PSD grain size, *Geophys. J. R. Astron. Soc., 71,* 497-518, 1982.

Heider, F., D. J. Dunlop, and N. Sugiura, Magnetic properties of hydrothermally recrystallized magnetite crystals, *Science, 236,* 1287-1289, 1987.

Heider, F., S. L. Halgedahl, and D. J. Dunlop, Temperature dependence of magnetic domains in magnetite crystals, *Geophys. Res. Lett., 15,* 499-502, 1988.

Heider, F., D. J. Dunlop, and H. C. Soffel, Low-temperature and alternating field demagnetization of saturation remanence and thermoremanence in magnetite grains (0.037 μm to 5 mm), *J. Geophys. Res., 97,* 9371-9381, 1992.

Johnson, H. P., W. Lowrie, and D. V. Kent, Stability of anhysteretic remanent magnetization in fine and coarse magnetite and maghemite particles, *Geophys. J. R. Astron. Soc., 41,* 1-10, 1975.

Lowrie, W, and M. Fuller, On the alternating field demagnetization characteristics of multidomain thermoremanent magnetization in magnetite, *J. Geophys. Res., 76,* 6339-6349, 1971.

Moon, T., and R. T. Merrill, Magnetic screening in multidomain material, *J. Geomagn. Geoelectr., 38,* 883-894, 1986.

Moskowitz, B. M., Micromagnetic study of the influence of crystal defects on coercivity in magnetite, *J. Geophys. Res., 98,* 18,011-18,026, 1993.

Néel, L., Some theoretical aspects of rock magnetism, *Adv. Phys., 4,* 191-242, 1955.

Özdemir, Ö., and D. J. Dunlop, Magnetic domain structures on a natural single crystal of magnetite, *Geophys. Res. Lett., 20,* 1835-1838, 1993.

Parry, L. G., Magnetic properties of dispersed magnetite powders, *Philos. Mag., 11,* 303-312, 1965.

Rimbert, F., Contribution à l'étude de l'action de champs alternatifs sur les aimantations rémanentes des roches. Applications géophysiques, *Rev. Inst. Fr. Pétr. Ann. Comb. Liq., 14,* 17-54, 123-155, 1959.

Schmidt, V. A., A multidomain model of thermoremanence, *Earth Planet. Sci. Lett., 20,* 440-446, 1973.

Schmidt, V. A., The variation of the blocking temperature in models of thermoremanence (TRM), *Earth Planet. Sci. Lett., 29,* 146-154, 1976.

Stacey, F. D., A generalized theory of thermoremanence, covering the transition from single domain to multidomain magnetic grains, *Philos. Mag., 7,* 1887-1900, 1962.

Stacey, F. D., The physical theory of rock magnetism, *Adv. Phys., 12,* 45-133, 1963.

Xu, S., Microcoercivity and bulk coercivity in multidomain grains, Ph.D. thesis, Univ. of Wash., Seattle, 1989.

Xu, S., and D. J. Dunlop, Theory of alternating field demagnetization of multidomain grains and implications for the origin of pseudo-single-domain remanence, *J. Geophys. Res., 98,* 4183-4190, 1993.

Xu, S., and R. T. Merrill, Microstress and microcoercivity, *J. Geophys. Res. 94,* 10,627-10,636, 1989.

Xu, S., and R. T. Merrill, Microcoercivity, bulk coercivity and saturation remanence in multidomain materials, *J. Geophys. Res., 95,* 7083-7090, 1990.

Xu, S., and R. T. Merrill, Stress, grain size and magnetic stability of magnetite, *J. Geophys. Res., 97,* 4321-4330, 1992.

D. J. Dunlop and S. Xu, Department of Physics, Erindale College, University of Toronto, 3359 Mississauga Road North, Mississauga, Ontario, Canada L5L 1C6. (e-mail: dunlop@physics.utoronto.ca)

(Received October 14, 1994; revised June 27, 1995;
accepted July 6, 1995.)